

1 **A genetically encoded GRAB sensor for measuring**
2 **serotonin dynamics *in vivo***

3

4 Jinxia Wan^{1,2}, Wanling Peng³, Xuelin Li^{1,2}, Tongrui Qian^{1,2}, Kun Song³, Jianzhi Zeng^{1,2,4},
5 Fei Deng^{1,2}, Suyu Hao^{1,2}, Jiesi Feng^{1,2,4}, Peng Zhang⁵, Yajun Zhang⁵, Jing Zou^{1,2,6}, Sunlei
6 Pan^{1,2,4}, J. Julius Zhu^{5,7,8}, Miao Jing^{1,2,4,9}, Min Xu³, Yulong Li^{1,2,4,*}

7

8 ¹State Key Laboratory of Membrane Biology, Peking University School of Life Sciences,
9 Beijing 100871, China

10 ²PKU-IDG/McGovern Institute for Brain Research, Beijing 100871, China

11 ³Institute of Neuroscience, State Key Laboratory of Neuroscience, CAS Center for
12 Excellence in Brain Science and Intelligence Technology, Chinese Academy of Sciences,
13 Shanghai 200031, China

14 ⁴Peking-Tsinghua Center for Life Sciences, Academy for Advanced Interdisciplinary
15 Studies, Peking University, Beijing 100871, China

16 ⁵Department of Pharmacology, University of Virginia School of Medicine, Charlottesville,
17 VA 22908, USA

18 ⁶Department of Biological Sciences, Neurobiology Section, University of Southern
19 California, Los Angeles, CA 90089, USA

20 ⁷School of Medicine, Ningbo University, Ningbo 315010, China

21 ⁸Donders Institute for Brain, Cognition and Behavior, Radboud University Nijmegen, 6525
22 EN, Nijmegen, Netherlands

23 ⁹Chinese Institute for Brain Research, Beijing 102206, China

24

25 *Manuscript correspondence:

26 Yulong Li (yulongli@pku.edu.cn)

27

28 **Abstract**

29 Serotonin (5-HT) is a phylogenetically conserved monoamine neurotransmitter modulating
30 a variety of processes in the brain. To directly visualize the dynamics of 5-HT, we developed
31 a genetically encoded GPCR-Activation-Based 5-HT (GRAB_{5-HT}) sensor with high
32 sensitivity, selectivity, and spatiotemporal resolution. GRAB_{5-HT}, detected 5-HT release in
33 multiple physiological and pathological conditions in both flies and mice, and thus provides
34 new insights into the dynamics and mechanisms of 5-HT signaling.

35 **Main**

36 Serotonergic signaling in the brain plays a critical role in a wide range of physiological
37 processes, including mood control, reward processing, and sleep-wake homeostatic
38 regulation¹⁻³. Given its functional importance, drugs targeting central serotonergic activity
39 have been used to treat virtually every psychiatric disorder, with the best example being
40 the use of selective serotonin reuptake inhibitors (SSRIs) for depression⁴. Despite the
41 importance of 5-HT, understanding of cell-specific 5-HT signaling during behaviors is
42 greatly hampered by the lack of ability to measure 5-HT *in vivo* with high sensitivity and
43 precise spatiotemporal resolution^{5,6,7}. Using molecular engineering, we developed a
44 genetically encoded fluorescent sensor for directly measuring extracellular 5-HT.

45 Previously, we and others independently developed GPCR activation based sensors for
46 detecting different neurotransmitters by converting the conformational change in the
47 respective GPCR to a sensitive fluorescence change in circularly permuted GFP (cpGFP)⁸.
48 ^{9,10,11}. Using similar strategy, we initiated the engineering of 5-HT-specific GRAB sensor
49 by inserting a cpGFP into the third intracellular loop (ICL3) of various 5-HT receptors.
50 Based on the performance of membrane trafficking and affinity of receptor-cpGFP
51 chimeras, we selected and focused on the 5-HT_{2C} receptor-based chimera for further
52 optimization (Extended Data Fig. 1a,b). Mutagenesis and screening in its linker regions
53 and cpGFP moiety, resulted in a sensor with a 250% $\Delta F/F_0$ in response to 5-HT, which we
54 named GRAB_{5-HT1.0} (referred to hereafter as simply 5-HT1.0; Fig 1a and Extended Data
55 Fig. 2). In addition, we generated a 5-HT-insensitive version of this sensor by introducing
56 the D134^{3,32}Q mutation in the receptor¹², resulting in GRAB_{5-HTmut} (referred to hereafter as
57 5-HTmut). This mutant sensor has the similar membrane trafficking as 5-HT1.0, but <2%
58 $\Delta F/F_0$ even in response to 100 μ M 5-HT (Fig. 1a and Extended Data Fig. 3a-d). In cultured
59 neurons, the 5-HT1.0 sensor produced a robust fluorescence increase (280% $\Delta F/F_0$) in
60 both the soma and neurites in response to 5-HT application, whereas 5-HTmut sensor had
61 no measurable change in fluorescence (Fig. 1b and Extended Data Fig. 3I).

62 Next, we characterized the properties of the 5-HT1.0 sensor, including the brightness and
63 photostability, dose-response relationship between 5-HT concentration and fluorescence
64 change, response kinetics, signal specificity and downstream coupling. We found that the
65 5-HT1.0 had similar brightness and better photostability compared to EGFP (Extended
66 Data Fig. 3e-g). In addition, we measured the sensor's kinetics upon application of 5-HT
67 (to measure the on-rate) followed by the 5-HT receptor antagonist metergoline (Met, to
68 measure the off-rate) and measured τ_{on} and τ_{off} values to be 0.2 s and 3.1 s, respectively
69 (Fig. 1c). The 5-HT1.0 was highly sensitive to 5-HT, with an EC₅₀ of 22 nM (Fig. 1e).

70 Importantly, none of other neurotransmitters and neuromodulators tested elicited a
71 detectable fluorescence change, and the 5-HT-induced signal was eliminated by the 5-HT
72 receptor antagonist SB 242084 (SB) (Fig. 1d and Extended Data Fig. 3m,n), indicating a
73 high specificity to 5-HT. Unlike the native 5-HT_{2C} receptor, which couples to the intracellular
74 G-protein and β -arrestin signaling pathways, the 5-HT1.0 sensor showed no detectable
75 coupling to either of these two pathways measured by the calcium imaging, G-protein-
76 dependent luciferase complementation assay¹³, TANGO assay¹⁴, and long-term
77 measurements of membrane fluorescence in the presence of 5-HT (Fig. 1f,g and Extended
78 Data Fig. 3h-k).

79 Next, we measured the dynamics of endogenous 5-HT upon neuronal activation. We
80 expressed either 5-HT1.0 or 5-HTmut in the mouse dorsal raphe nucleus (DRN) by AAV,
81 and prepared acute brain slices three weeks after infection (Fig. 2a). In DRN slices
82 expressing 5-HT1.0, a single electrical pulse evoked detectable fluorescence increases,
83 and the response progressively enhanced with the increase in pulse number or frequency
84 (Fig. 2b,c and Extended Data Fig. 4a). The stimulation evoked-response was repeatable
85 for up to 25 min (Extended Data Fig. 4b) and blocked by the 5-HT receptor antagonist Met,
86 but not the dopamine receptor antagonist haloperidol (Halo; Fig. 2d and Extended Data
87 Fig. 4c,d). In contrast, the same electrical stimuli had no effect on fluorescence in slices
88 expressing the 5-HTmut sensor (Fig. 2b,d). We also measured the kinetics of the
89 fluorescence change in response to 100 ms electrical stimulation and found τ_{on} and τ_{off}
90 values of 0.15 s and 7.22 s (Fig. 2e). We further compared the 5-HT1.0 sensor with existing
91 fast-scan cyclic voltammetry (FSCV) in recording 5-HT by simultaneously conducting
92 fluorescence imaging and electrochemical recording in DRN slices (Fig. 2f). Both methods
93 could sensitively detect single pulse-evoked 5-HT signal and the increase of response
94 following incremental frequencies (Fig. 2g and Extended Data Fig. 4e,f). Importantly, the
95 5-HT1.0 showed better signal to noise ratio (SNR) compared with FSCV (Fig. 2g).

96 We next tested whether the 5-HT1.0 sensor could be used to measure sensory-relevant
97 changes in 5-HT signaling *in vivo*. We used the *Drosophila* model, as serotonergic
98 signaling in the mushroom body (MB) has been implicated in odor-related memory
99 consolidation¹⁵, in which 5-HT is released from single serotonergic dorsal paired medial
100 (DPM) neurons that innervate Kenyon cells (KC) in the MB per hemisphere^{16, 17}. The 5-
101 HT1.0 reliably reported 5-HT release evoked by electrically stimulating the horizontal lobe
102 of MB, revealing rapid on and off kinetics of 0.07 s and 4.08 s, respectively. Moreover, the
103 signal was blocked by applying Met (Fig. 2h-j and Extended Data Fig. 4g-i). Two distinct
104 physiological stimuli—odor application and body shock—evoked a robust fluorescence
105 increase in the MB β' lobe of flies (Fig. 2k-p and Extended Data movie 1), consistent with
106 previous studies of Ca²⁺ signaling in the DPM¹⁸. In contrast, no fluorescence changes
107 detected in flies expressing the 5-HTmut sensor (Fig. 2k-p, Extended Data movie 1).
108 Neither stimulus produced a saturated response of 5-HT1.0 sensor, as application of
109 exogenous 100 μ M 5-HT in the same flies elicited much larger responses. Finally, co-
110 expressing the 5-HT1.0 sensor together with red fluorescent Ca²⁺ sensor jRCaMP1a in KC
111 to perform two-color imaging to examine whether the expression of the 5-HT1.0 sensor
112 affects the odorant-evoked Ca²⁺ response. Both 5-HT1.0 and jRCaMP1a produced highly

113 sensitive fluorescence increases in response to the odorant application in the green and
114 red channels, respectively (Fig. 2q-s and Extended Data Fig. 4j-l). Importantly, jRCaMP1a-
115 expressing flies with or without co-expression of 5-HT1.0 had similar odorant-evoked Ca^{2+}
116 signals, suggesting virtually no effect of expressing the 5-HT1.0 sensor on cellular
117 physiology (Fig. 2q-s and Extended Data Fig. 4j-l).

118 Methylenedioxymethamphetamine (MDMA) is a synthetic addictive compound which could
119 alter mood and perception, and its effects can be partially explained by increasing
120 extracellular 5-HT concentrations in the brain¹⁹. We examined MDMA's effect *in vivo* by
121 two-photon imaging in mice expressing the sensor in the prefrontal cortex (PFC) (Fig. 3a).
122 Intraperitoneal (i.p.) injection of MDMA caused a progressive increase in 5-HT1.0
123 fluorescence, which peaked after 1 hour and then gradually decayed over the following 3
124 hours (Fig. 3b-d). The time course is comparable with previous reports of MDMA's effects
125 on both human²⁰ and mouse²¹. Meanwhile, MDMA had no effect on fluorescence of 5-
126 HTmut sensor (Fig. 3a-d). These results together suggest that the 5-HT1.0 sensor is
127 suitable for stable, long-term imaging *in vivo*.

128 Finally, we examined whether the 5-HT1.0 sensor could measure the dynamics of
129 serotonergic activity under physiological conditions, e.g. the sleep-wake cycle in mice. The
130 5-HT1.0 sensor was expressed in several brain nuclei, including the basal forebrain (BF),
131 orbital frontal cortex (OFC), and the bed nucleus of the stria terminalis (BNST), then we
132 performed simultaneous fiber-photometry and EEG/EMG recordings in freely behaving
133 mice. In BF, we found that the 5-HT1.0 sensor signal was generally higher when the mice
134 were awake compared to either REM or non-REM (NREM) sleep, with the lowest signal
135 detected during REM sleep, consistent with the notion that 5-HT signaling is minimum
136 during REM sleep²² (Fig. 3e-g). As expected, we found no significant change in
137 fluorescence in mice expressing 5-HTmut sensor during the sleep-wake cycle. Interestingly,
138 simultaneous recording 5-HT1.0 in OFC and BNST revealed tight correlation in
139 fluorescence during NREM sleep (Fig. 3h,i), suggesting global synchrony of the 5-HT
140 signaling despite of the region-specific innervation by different subpopulations of the
141 serotonergic neurons in DRN^{23, 24}. Lastly, consistent with our previous findings, we found
142 that treating mice with the 5-HT receptor antagonist Met largely blocked the fluorescence
143 change of the 5-HT1.0 sensor (Fig. 3j,k), validating the specificity of measured signals *in*
144 *vivo*.

145 In summary, we report the development and application of a novel genetically encoded
146 fluorescent GRAB sensor for measuring extracellular 5-HT dynamics. This GRAB_{5-HT1.0}
147 sensor has high sensitivity and specificity, as well as high spatiotemporal resolution, yet it
148 does not appear to affect cellular physiology. GRAB_{5-HT1.0} reliably reports endogenous 5-
149 HT release in response to a variety of stimuli and under various behaviors in different
150 animal models. GRAB_{5-HT1.0} follows 5-HT dynamics in mice throughout the sleep-wake
151 cycle, providing new insights into the functional contribution of 5-HT in sleep regulation.

152

153 **Methods**

154 **Primary cultures**

155 Male and female postnatal day 0 (P0) Sprague-Dawley rat pups were obtained from
156 (Beijing Vital River) and used to prepare cortical neurons. The cortex was dissected, and
157 neurons were dissociated using 0.25% Trypsin-EDTA (GIBCO), plated on 12-mm glass
158 coverslips coated with poly-D-lysine (Sigma-Aldrich), and cultured in neurobasal medium
159 (GIBCO) containing 2% B-27 supplement (GIBCO), 1% GlutaMax (GIBCO), and 1%
160 penicillin-streptomycin (GIBCO). The neurons were cultured at 37°C in a humidified
161 atmosphere in air containing 5% CO₂.

162 **Cell lines**

163 HEK293T cells were purchased from ATCC and verified based on their morphology under
164 microscopy and an analysis of their growth curve. Stable cell lines expressing either 5-
165 HT_{2C} or 5-HT1.0 were generated by co-transfecting cells with the pPiggyBac plasmid
166 carrying the target genes together with Tn5 transposase into a stable HEK293T cell line.
167 Cells expressing the target genes were selected using 2 µg/ml Puromycin (Sigma). An
168 HEK293 cell line stably expressing a tTA-dependent luciferase reporter and the β-
169 arrestin2-TEV fusion gene used in the TANGO assay was a generous gift from Bryan L.
170 Roth²⁵. All cell lines were cultured at 37°C in 5% CO₂ in DMEM (GIBCO) supplemented
171 with 10% (v/v) fetal bovine serum (GIBCO) and 1% penicillin-streptomycin (GIBCO).

172 **Drosophila**

173 UAS-GRAB_{5-HT1.0} (attp40, UAS-GRAB_{5-HT1.0}/CyO) and UAS-GRAB_{5-HTmut} (attp40, UAS-
174 GRAB_{5-HTmut}/CyO) flies were generated in this study. The coding sequences of GRAB_{5-HT1.0}
175 or GRAB_{5-HTmut} were inserted into pJFRC28²⁶ (Addgene plasmid #36431) using Gibson
176 assembly. These vectors were injected into embryos and integrated into attp40 via PhiC31
177 by the Core Facility of Drosophila Resource and Technology, Shanghai Institute of
178 Biochemistry and Cell Biology, Chinese Academy of Sciences. The following fly stocks
179 were used in this study: R13F02-Gal4 (BDSC:49032) and UAS-jRCaMP1a (BDSC:
180 63792)²⁷. Flies were raised on standard cornmeal-yeast medium at 25°C, with 70% relative
181 humidity and a 12h/12h light/dark cycle. In Fig. 2h-p and Extended Data Fig.4g-i, fly UAS-
182 GRAB_{5-HT1.0}/CyO; R13F02-Gal4/TM2 and fly UAS-GRAB_{5-HTmut}/+; R13F02-Gal4/+ were
183 used; in Fig. 2q-s and Extended Data Fig.4j-l, fly UAS-GRAB_{5-HT1.0}/+; R13F02-Gal4/UAS-
184 jRCaMP1a/+ and fly R13F02-Gal4/UAS-jRCaMP1a were used.

185 **Mouse**

186 Wild-type C57BL/6 (P25-60) mice were used to prepare the acute brain slices and for the
187 *in vivo* mouse experiments. All mice were group-housed in a temperature-controlled room
188 with a 12h/12h light/dark cycle, with food and water provided ad libitum. All procedures for
189 animal surgery and maintenance were performed using protocols that were approved by
190 the Animal Care & Use Committees at Peking University, the Chinese Academy of
191 Sciences, University of Virginia, and were performed in accordance with the guidelines
192 established by the US National Institutes of Health.

193 **Molecular biology**

194 Plasmids were generated using the Gibson assembly method²⁸, and DNA fragments were
195 amplified by PCR using primers (Thermo Fisher Scientific) with 25-30 bp overlap. DNA
196 fragments were assembled using T5-exonuclease (New England Biolabs), Phusion DNA
197 polymerase (Thermo Fisher Scientific), and Taq ligase (iCloning). Sanger sequencing was
198 performed at the Sequencing Platform in the School of Life Sciences of Peking University
199 to verify plasmid sequences. cDNAs encoding various 5-HT receptors (5-HT_{1E}, 5-HT_{2C}, 5-
200 HT_{5A}, and 5-HT₆) were generated using PCR amplification of the full-length human GPCR
201 cDNA library (hORFeome database 8.1). For optimizing the 5-HT sensor, cDNAs encoding
202 the candidates in step 1 and step 2 were cloned into the pDisplay vector (Invitrogen) with
203 an IgK leader sequence in the sensor upstream. In step 3, in addition to upstream IgK
204 peptide, IRES-mCherry-CAAX cascade was fused downstream of the sensor to calibrate
205 the membrane signal. For optimizing the linker sequence and cpGFP, site-directed
206 mutagenesis was performed using primers containing NNB codons (48 codons, encoding
207 20 possible amino acids). For characterization in neurons, GRAB_{5-HT1.0} and GRAB_{5-HTmut}
208 were cloned into the pAAV vector under the hSyn, TRE, or CAG promoter. In downstream
209 coupling experiments, the GRAB_{5-HT} sensor and the 5-HT_{2C} receptor were cloned into the
210 pTango and pPiggyBac vectors, respectively; two mutations were introduced into pCS7-
211 PiggyBAC to generate hyperactive piggyBac transposase (ViewSolid Biotech)²⁹. The
212 GRAB_{5-HT1.0}-SmBit and 5-HT_{2C}-SmBit constructs were derived from β 2AR-SmBit¹³ using a
213 BamHI site incorporated upstream of the GGSG linker. LgBit-mGq was a generous gift
214 from Nevin A. Lambert.

215 **Expression of GRAB_{5-HT} in cultured cells and *in vivo***

216 HEK293T cells were plated on 12-mm glass coverslips in 24-well plates and grown to 70%
217 confluence for transfection with PEI (1 mg DNA and 3 mg PEI per well); the medium was
218 replaced after 4-6 hours, and cells were used for imaging 24 hours after transfection.
219 Cultured neurons were infected with AAVs expressing TRE-GRAB_{5-HT1.0} (titer: 3.8×10^{13}
220 particles/ml) and hSyn-tTA (titer: 1.3×10^{14} particles/ml) or hSyn-GRAB_{5-HTmut} (titer:
221 1×10^{13} particles/ml) at 7-9 DIV, and imaging was performed 7-14 days after infection.

222 For *in vivo* expression, mice were deeply anesthetized with an i.p. injection of 2,2,2-
223 tribromoethanol (Avertin, 500 mg/kg, Sigma-Aldrich) or ketamine (10 mg/kg) and xylazine
224 (2 mg/kg), placed in a stereotaxic frame, and the AAVs were injected using a microsyringe
225 pump (Nanoliter 2000 Injector, WPI). For the experiments shown in Fig. 2a-e and Extended
226 Data Fig. 4a-d, AAVs expressing CAG-GRAB_{5-HT1.0} (titer: 1.3×10^{13} particles/ml) or hSyn-
227 GRAB_{5-HTmut} (titer: 1×10^{13} particles/ml) were injected (volume: 400 nl) into the DRN at the
228 following coordinates relative to Bregma: AP: -4.3 mm, ML: 1.1 mm (depth: 2.85 mm, with
229 a 20° ML angle). For the experiments shown in Fig. 2f,g and Extended Data Fig. 4e,f,
230 Sindbis virus expressing GRAB_{5-HT1.0} was injected (volume: 50 nl) into the DRN at the
231 following coordinates relative to Bregma: AP: -4.3 mm, ML: 0.0 mm (depth: 3.00 mm). For
232 the experiments shown in Fig. 3a-d, AAVs expressing hSyn-GRAB_{5-HT1.0} (titer: 4.6×10^{13}
233 particles/ml) or hSyn-GRAB_{5-HTmut} (titer: 1×10^{13} particles/ml) were injected (volume: 400
234 nl) into the PFC at the following coordinates relative to Bregma: AP: +2.8 mm, ML: 0.5 mm

235 (depth: 0.5 mm). For the experiments shown in Fig. 3e-k, AAVs expressing CAG-GRAB_{5-HT1.0}
236 HT1.0 or hSyn-GRAB_{5-HTmut} were injected (volume: 400 nl) into the BF at the following
237 coordinates relative to Bregma: AP: 0 mm, ML: 1.3 mm (depth: 5.0 mm), the OFC (AP:
238 +2.6 mm, ML: 1.7 mm, depth: 1.7 mm), and the BNST (AP: +0.14 mm, ML: 0.8 mm, depth:
239 3.85 mm).

240 **Fluorescence imaging of HEK293T cells and cultured neurons**

241 An inverted Ti-E A1 confocal microscope (Nikon) combined with an Opera Phenix high-
242 content screening system (PerkinElmer) were used for imaging. The confocal microscope
243 was equipped with a 40x/1.35 NA oil-immersion objective, a 488-nm laser, and a 561-nm
244 laser. The GFP signal was collected using a 525/50-nm emission filter, and the RFP signal
245 was collected using a 595/50-nm emission filter. Cultured cells expressing GRAB_{5-HT1.0} or
246 GRAB_{5-HTmut} were either bathed or perfused with Tyrode's solution containing (in mM): 150
247 NaCl, 4 KCl, 2 MgCl₂, 2 CaCl₂, 10 HEPES, and 10 glucose (pH 7.4). Drugs were delivered
248 via a custom-made perfusion system or via bath application. The chamber was cleaned
249 thoroughly between experiments using 75% ethanol. Photostability was measured using
250 confocal microscopy (1-photon illumination) with the 488-nm laser at a laser power of 350
251 μ W, and the Opera Phenix high-content screening system was equipped with a 40x/1.1
252 NA water-immersion objective, a 488-nm laser, and a 561-nm laser; the GFP signal was
253 collected using a 525/50-nm emission filter, and the RFP signal was collected with a
254 600/30-nm emission filter. For imaging, the culture medium was replaced with 100 μ l of
255 Tyrode's solution, and drugs (at various concentrations) were applied in Tyrode's solution.
256 The fluorescence signal of the GRAB_{5-HT} sensors was calibrated using the GFP/RFP ratio.

257 **TANGO assay**

258 5-HT at various concentrations was applied to 5-HT_{2C}-expressing or 5-HT_{1.0}-expressing
259 HTLA cells²⁵. The cells were then cultured for 12 h to allow expression of firefly luciferase
260 (Fluc). Bright-Glo reagent (Fluc Luciferase Assay System, Promega) was then added to a
261 final concentration of 5 μ M, and luminescence was measured using a Victor X5 multilabel
262 plate reader (PerkinElmer).

263 **Luciferase complementation assay**

264 The luciferase complementation assay was performed as previously described¹³. In brief,
265 48 h after transfection the cells were washed with PBS, harvested by trituration, and
266 transferred to opaque 96-well plates containing 5-HT at various concentrations. Furimazine
267 (NanoLuc Luciferase Assay, Promega) was then added quickly to each well, followed by
268 measurement with Nluc.

269 **Fluorescence imaging of GRAB_{5-HT} in brain slices**

270 AAVs or Sindbis virus expressing GRAB_{5-HT1.0} or GRAB_{5-HTmut} were injected into the mouse
271 DRN as described above. Three weeks after AAV injection or 18 hours after Sindbis virus
272 injection, the mice were deeply anesthetized by an i.p. injection of Avertin or xylazine-
273 ketamine and then transcardially perfused with 10 ml oxygenated slicing buffer consisting
274 of (in mM): 110 choline-Cl, 2.5 KCl, 1 NaH₂PO₄, 25 NaHCO₃, 7 MgCl₂, 25 glucose, and 0.5

275 CaCl₂. The mice were then decapitated, and the brains were removed and placed in cold
276 (0-4°C) oxygenated slicing buffer for an additional 1 min. The brains were then rapidly
277 mounted on the cutting stage of a VT1200 vibratome (Leica) for coronal sectioning at 300
278 μm thickness. The brain slices containing the DRN were initially allowed to recover for ≥40
279 min at 34°C in oxygen-saturated Ringer's buffer consisting of (in mM): 125 NaCl, 2.5 KCl,
280 1 NaH₂PO₄, 25 NaHCO₃, 1.3 MgCl₂, 25 glucose, and 2 CaCl₂. For two-photon imaging, the
281 slices were transferred to a recording chamber that was continuously perfused with 34°C
282 oxygen-saturated Ringer's buffer and placed in an FV1000MPE two-photon microscope
283 (Olympus) equipped with a 25x/1.05 NA water-immersion objective. 5-HT1.0 or 5-HTmut
284 fluorescence was excited using a mode-locked Mai Tai Ti:Sapphire laser (Spectra-Physics)
285 at a wavelength of 920-nm and collected via a 495-540-nm filter. For electrical stimulation,
286 a bipolar electrode (cat. WE30031.0A3, MicroProbes) was positioned near the DRN in the
287 slice, and imaging and stimulation were synchronized using an Arduino board with a
288 custom-written program. The parameters of the frame scan were set to a size of 128 × 96
289 pixels with a speed of 0.1482 s/frame for electrical stimulation and a size of 512 × 512
290 pixels with a speed of 1.109 s/frame for drug perfusion experiments. For the kinetics
291 measurements, line scans were performed with a rate of 800-850 Hz. The stimulation
292 voltage was set at 4-6 V, and the duration of each stimulation was set at 1 ms. Drugs were
293 bath-applied by perfusion into the recording chamber in pre-mixed Ringer's buffer. For the
294 Sindbis virus infected mouse brain slices, wide-field epifluorescence imaging was
295 performed using Hamamatsu ORCA FLASH4.0 camera (Hamamatsu Photonics, Japan),
296 and 5-HT1.0-expressing cells in acutely prepared brain slices are excited by a 460-nm
297 ultrahigh-power low-noise LED (Prizmatix, Givat-Shmuel, Israel). The frame rate of
298 FLASH4.0 camera was set to 10 Hz. To synchronize image capture with electrical
299 stimulation, and fast-scan cyclic voltammetry, the camera was set to external trigger mode
300 and triggered by a custom-written IGOR Pro 6 program (WaveMetrics, Lake Oswego, OR).
301 For electrical stimulation, a home-made bipolar electrode was positioned near the DRN in
302 the slice and the stimulation current was set at 350 μA and the duration of each stimulation
303 was set at 1 ms.

304 **Fast-scan cyclic voltammetry (FSCV)**

305 Carbon-fiber microelectrodes (CFME) were fabricated as described previously³⁰. Briefly,
306 cylindrical CFMEs (7 μm in radius) were constructed with T-650 carbon fiber (Cytec
307 Engineering Materials) which was aspirated into a glass capillary (1.2 mm O.D and 0.68
308 mm I.D, A-M system) and pulled using the PE-22 puller (Narishige Int.). The carbon fiber
309 was trimmed to 50 to 70 μm in length from the pulled glass tip and sealed with epoxy which
310 was cured at 100 °C for 2 hours followed by 150 °C overnight. CFMEs were cleaned in
311 isopropyl alcohol for 30 min prior to the Nafion electrodeposition. Nafion was
312 electrochemically deposited by submerging CFME tip in Nafion® solution (5 wt% 1100 EW
313 Nafion® in methanol, Ion Power), and a constant potential of 1.0 V vs Ag/AgCl was applied
314 to the electrode for 30 seconds. Then, Nafion coated electrodes were air dried for 10
315 seconds, and then at 70 °C for 10 minutes. For electrochemical detection of 5-HT, a
316 Jackson waveform was applied to the electrode by scanning the potential from 0.2 V to 1.0
317 V to – 0.1 V and back to 0.2 V at 1000 V/s using a ChemClamp potentiostat (Dagan). For

318 data collection and analysis, TarHeel (provided by R.M. Wightman, University of North
319 Carolina) was used. For the electrode calibrations, phosphate buffer (PBS) solution was
320 used which consisting of (in mM): 131.25 NaCl, 3.0 KCl, 10.0 NaH₂PO₄, 1.2 MgCl₂, 2.0
321 Na₂SO₄, and 1.2 CaCl₂ (pH 7.4). A 5-HT stock solution was prepared in 0.1 M HClO₄ and
322 diluted to 500 nM with PBS for calibrations prior to the experiment.

323 **Fluorescence imaging of transgenic flies**

324 Fluorescence imaging in flies was performed using an Olympus two-photon microscope
325 FV1000 equipped with a Spectra-Physics Mai Tai Ti:Sapphire laser. A 930-nm excitation
326 laser was used for one-color imaging of 5-HT1.0 or 5-HTmut, and a 950-nm excitation laser
327 was used for two-color imaging with 5-HT1.0 and jRCaMP1a. For detection, 495-540-nm
328 filter for green channel and 575-630-nm filter for red channel. Adults male flies within 2
329 weeks post eclosion were used for imaging. To prepare the fly for imaging, adhesive tape
330 was affixed to the head and wings. The tape above the head was excised, and the chitin
331 head shell, air sacs, and fat bodies were carefully removed to expose the central brain.
332 The brain was bathed continuously in adult hemolymph-like solution (AHLS) composed of
333 (in mM): 108 NaCl, 5 KCl, 5 HEPES, 5 trehalose, 5 sucrose, 26 NaHCO₃, 1 NaH₂PO₄, 2
334 CaCl₂, and 1-2 MgCl₂. For electrical stimulation, a glass electrode (resistance: 0.2 MΩ)
335 was placed in proximity to the MB medial lobe, and voltage for stimulation was set at 10-
336 30 V. For odorant stimulation, the odorant isoamyl acetate (cat. 306967, Sigma-Aldrich)
337 was first diluted 200-fold in mineral oil, then diluted 5-fold with air, and delivered to the
338 antenna at a rate of 1000 ml/min. For body shock, two copper wires were attached to the
339 fly's abdomen, and a 500-ms electrical stimuli was delivered at 50-80 V. For 5-HT
340 application, the blood-brain barrier was carefully removed, and 5-HT was applied at a final
341 concentration 100 μM. An Arduino board was used to synchronize the imaging and
342 stimulation protocols. The sampling rate during electrical stimulation, odorant stimulation,
343 body shock stimulation, and 5-HT perfusion was 12 Hz, 6.8 Hz, 6.8 Hz, and 1 Hz
344 respectively.

345 **Two-photon imaging in mice**

346 Fluorescence imaging in mice was performed using an Olympus two-photon microscope
347 FV1000 equipped with a Spectra-Physics Mai Tai Ti:Sapphire laser. The excitation
348 wavelength was 920-nm, and fluorescence was collected using a 495-540-nm filter. To
349 perform the imaging in head-fixed mice, part of the mouse scalp was removed, and the
350 underlying tissues and muscles were carefully removed to expose the skull. A metal
351 recoding chamber was affixed to the skull surface with glue followed by a thin layer of
352 dental cement to strengthen the connection. One to two days later, the skull above the
353 prefrontal cortex was carefully removed, taking care to avoid the major blood vessels. AAVs
354 expressing GRAB_{5-HT1.0} or GRAB_{5-HTmut} was injected as above described. A custom-made
355 4 mm x 4 mm square coverslip was placed over the exposed PFC and secured with glue.
356 After surgery, mice were allowed to recover for at least three weeks. The mice were then
357 fixed to the base and allowed to habituate for 2-3 days. During the experiment, drugs were
358 administered by i.p. injection, and the sampling rate was 0.1 Hz.

359

360 **Fiber-photometry recording in mice**

361 To monitor 5-HT release in various brain regions during the sleep-wake cycle, AAVs
362 expressing GRAB_{5-HT1.0} or GRAB_{5-HTmut} were injected via a glass pipette into the BF, OFC,
363 and BNST using a Nanoject II (Drummond Scientific). An optical fiber (200 μm , 0.37 NA)
364 with FC ferrule was carefully inserted at the same coordinates used for virus injection. The
365 fiber was affixed to the skull surface using dental cement. After surgery, the mice were
366 allowed to recover for at least one week. The photometry rig was constructed using parts
367 obtained from Doric Lens, including a fluorescence optical mini cube
368 (FMC4_AE(405)_E(460-490)_F(500-550)_S), a blue LED (CLED_465), an LED driver
369 (LED_2), and a photo receiver (NPM_2151_FOA_FC). To record GRAB_{5-HT1.0} and GRAB₅₋
370 _{HTmut} fluorescence signals, a beam of excitation light was emitted from an LED at 20 μW ,
371 and the optical signals from GRAB_{5-HT1.0} and GRAB_{5-HTmut} were collected through optical
372 fibers. For the fiber-photometry data, a software-controlled lock-in detection algorithm was
373 implemented in the TDT RZ2 system using the fiber-photometry “Gizmo” in the Synapse
374 software program (modulation frequency: 459 Hz; low-pass filter for demodulated signal:
375 20 Hz, 6th order). The photometry data were collected with a sampling frequency of 1017
376 Hz. The recording fiber was bleached before recording to eliminate autofluorescence from
377 the fiber, and the background fluorescence intensity was recorded and subtracted from the
378 recorded signal during data analysis.

379 **EEG and EMG recordings**

380 Mice were anesthetized with isoflurane (5% induction; 1.5-2% maintenance) and placed
381 on a stereotaxic frame with a heating pad. For EEG, two stainless steel miniature screws
382 were inserted in the skull above the visual cortex, and two additional steel screws were
383 inserted in the skull above the frontal cortex. For EMG, two insulated EMG electrodes were
384 inserted in the neck musculature, and a reference electrode was attached to a screw
385 inserted in the skull above the cerebellum. The screws in the skull were affixed using thick
386 dental cement. All experiments were performed at least one week after surgery. TDT
387 system-3 amplifiers (RZ2 and PZ5) were used to record the EEG and EMG signals; the
388 signal was passed through a 0.5-Hz high-pass filter and digitized at 1526 Hz.

389 **Quantification and statistical analysis**

390 Imaging data from cultured HEK293T cells, cultured neurons, acute brain slices, transgenic
391 flies, and head-fixed mice were processed using ImageJ software (NIH) and analyzed
392 using custom-written MATLAB programs. Traces were plotted using Origin 2018.
393 Exponential function fitting in Origin was used to correct for slight photobleaching of the
394 traces in Fig. 2i,m,n,o,r and Extended Data Fig. 4i,k. In Fig. 2l and Extended Data Fig. 4h,
395 the background levels measured outside the ROI of the pseudocolor images were removed
396 using ImageJ.

397 For the fiber-photometry data analysis, the raw data were binned into 1-Hz bins (i.e., down-
398 sampled by 1000) and background autofluorescence was subtracted. For calculating $\Delta F/F_0$,
399 a baseline value was obtained by fitting the autofluorescence-subtracted data with a 2nd
400 order exponential function. Slow drift was removed from the z-score-transformed $\Delta F/F_0$

401 using the MATLAB script “BEADS” with a cut-off frequency of 0.00035 cycles/sample
402 ([https://www.mathworks.com/matlabcentral/fileexchange/49974-beads-baseline-](https://www.mathworks.com/matlabcentral/fileexchange/49974-beads-baseline-estimation-and-denoising-with-sparsity)
403 [estimation-and-denoising-with-sparsity](https://www.mathworks.com/matlabcentral/fileexchange/49974-beads-baseline-estimation-and-denoising-with-sparsity)). To quantify the change in 5-HT fluorescence
404 across multiple animals, the z-score-transformed $\Delta F/F_0$ was further normalized using the
405 standard deviation of the signal measured during REM sleep (when there was no apparent
406 fluctuation in the signal), yielding a normalized z-score. This normalized z-score was used
407 for the analysis in Fig. 3e-k.

408 For EEG and EMG data analysis, Fast Fourier transform (FFT) was used to perform
409 spectral analysis with a frequency resolution of 0.18 Hz. Brain state was classified semi-
410 automatically in 5-s epochs using a MATLAB GUI and then validated manually by trained
411 experimenters. Wakefulness was defined as desynchronized EEG activity combined with
412 high EMG activity; NREM sleep was defined as synchronized EEG activity combined high-
413 amplitude delta activity (0.5-4 Hz) combined with low EMG activity; and REM sleep was
414 defined as high power at theta frequencies (6-9 Hz) combined with low EMG activity.

415 Except where indicated otherwise, all summary data are reported as the mean \pm s.e.m.
416 The signal to noise ratio (SNR) was calculated as the peak response divided by the
417 standard deviation of the baseline fluorescence. Group differences were analyzed using
418 the Student’s t-test, and differences with a p-value <0.05 were considered significant.
419 Cartoons in Fig. 3a,e,h,j are created with BioRender.com.

420

421 **Data and software availability**

422 The custom-written MATLAB and Arduino programs used in this study will be provided
423 upon request.

424

425 **Acknowledgments**

426 We thank Yi Rao for providing the two-photon microscope and Xiaoguang Lei for platform
427 support for the Opera Phenix high-content screening system at PKU-CLS. This work was
428 supported by the Beijing Municipal Science & Technology Commission
429 (Z181100001318002), the Beijing Brain Initiative of Beijing Municipal Science &
430 Technology Commission (Z181100001518004), Guangdong Grant “Key Technologies for
431 Treatment of Brain Disorders” (2018B030332001), the General Program of National
432 Natural Science Foundation of China (projects 31671118, 31871087, and 31925017), the
433 NIH BRAIN Initiative (NS103558), grants from the Peking-Tsinghua Center for Life
434 Sciences and the State Key Laboratory of Membrane Biology at Peking University School
435 of Life Sciences (to Y.L.), the Shanghai Municipal Science and Technology Major Project
436 (2018SHZDZX05 to M.X.), and the Shanghai Pujiang Program (18PJ1410800 to M.X.),
437 Alzheimer’s Association Postdoctoral Research Fellowship (P.Z.) and Peking-Tsinghua
438 Center Excellence Postdoctoral Fellowship (Y.Z.).

439

440 **Author contributions**

441 Y.L. conceived and supervised the project. J.W., M.J., F.D., S.H., J.F., J. Zou and S.P.
442 performed the experiments related to developing, optimizing, and characterizing the sensor
443 in cultured HEK293T cells and neurons. T.Q. performed the experiments using AAVs in
444 slices. X.L. and J.Z. performed the *Drosophila* experiments. P.Z. and Y.Z. performed the
445 experiments using the Sindbis virus in slices under the supervision of J.J.Z. J.W. performed
446 the two-photon imaging in head-fixed mice. W.P. and K.S. performed the fiber-photometry
447 recordings in behaving mice under the supervision of M.X. All authors contributed to the
448 data interpretation and analysis. Y.L. and J.W. wrote the manuscript with input from all other
449 authors.

450

451 **Competing Interests**

452 The authors declare competing financial interests. J.W., M.J., J.F, and Y. L have filed patent
453 applications whose value might be affected by this publication.

454

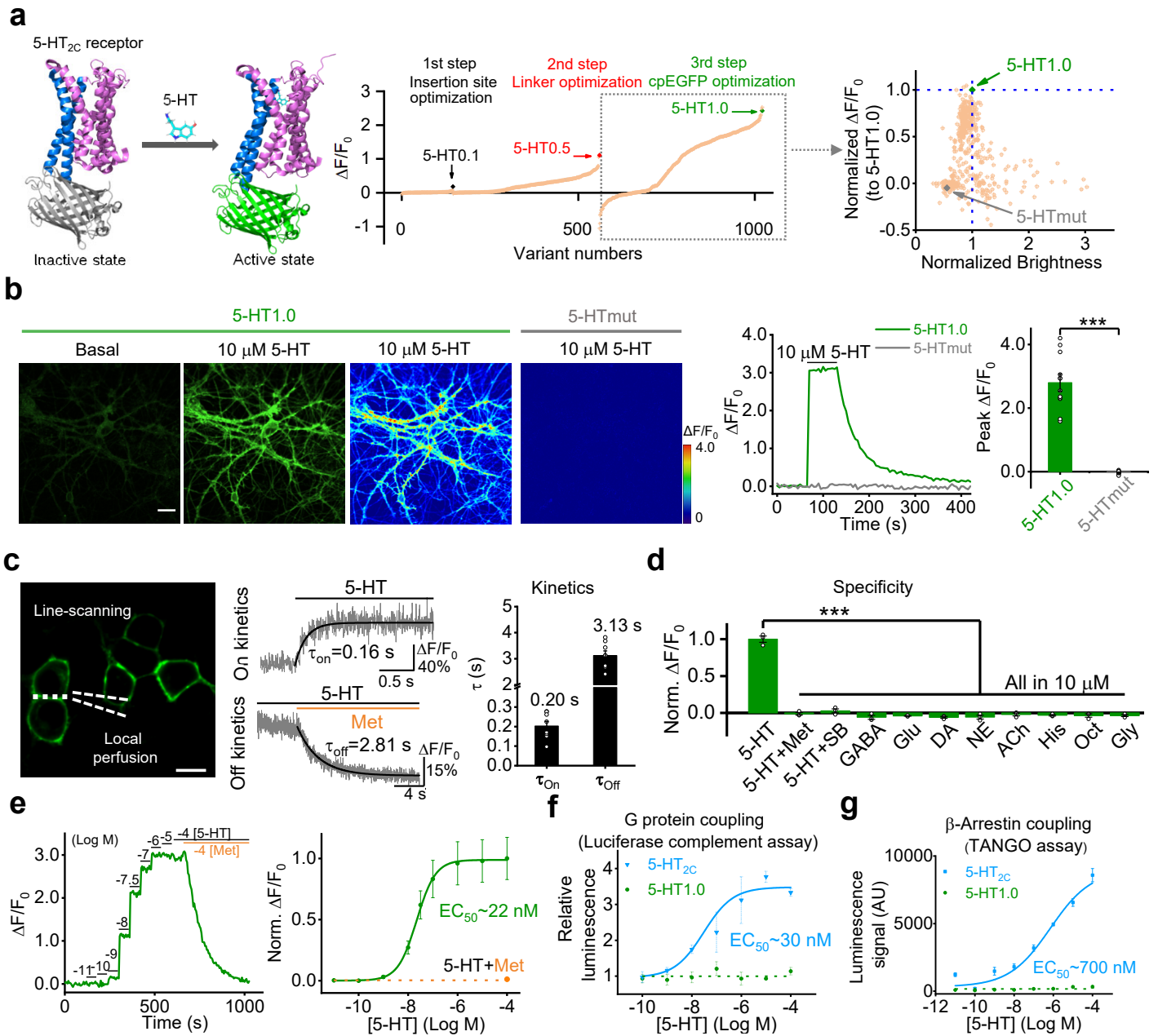
455 **References**

- 456 1. Lesch, K.P., *et al.* Association of anxiety-related traits with a polymorphism in the serotonin
457 transporter gene regulatory region. *Science* **274**, 1527-1531 (1996).
- 458 2. Li, Y., *et al.* Serotonin neurons in the dorsal raphe nucleus encode reward signals. *Nat*
459 *Commun* **7**, 10503 (2016).
- 460 3. Portas, C.M., *et al.* On-line detection of extracellular levels of serotonin in dorsal raphe
461 nucleus and frontal cortex over the sleep/wake cycle in the freely moving rat. *Neuroscience* **83**,
462 807-814 (1998).
- 463 4. Vaswani, M., Linda, F.K. & Ramesh, S. Role of selective serotonin reuptake inhibitors in
464 psychiatric disorders: a comprehensive review. *Prog Neuropsychopharmacol Biol Psychiatry*
465 **27**, 85-102 (2003).
- 466 5. Fuller, R.W. Uptake inhibitors increase extracellular serotonin concentration measured by
467 brain microdialysis. *Life Sci* **55**, 163-167 (1994).
- 468 6. Bunin, M.A., Prioleau, C., Mailman, R.B. & Wightman, R.M. Release and uptake rates of
469 5-hydroxytryptamine in the dorsal raphe and substantia nigra reticulata of the rat brain. *J*
470 *Neurochem* **70**, 1077-1087 (1998).
- 471 7. Candelario, J. & Chachisvilis, M. Mechanical Stress Stimulates Conformational Changes
472 in 5-Hydroxytryptamine Receptor 1B in Bone Cells. *Cellular and Molecular Bioengineering* **5**,
473 277-286 (2012).
- 474 8. Jing, M., *et al.* A genetically encoded fluorescent acetylcholine indicator for in vitro and in
475 vivo studies. *Nat Biotechnol* **36**, 726-737 (2018).
- 476 9. Patriarchi, T., *et al.* Ultrafast neuronal imaging of dopamine dynamics with designed
477 genetically encoded sensors. *Science* **360** (2018).
- 478 10. Sun, F., *et al.* A Genetically Encoded Fluorescent Sensor Enables Rapid and Specific
479 Detection of Dopamine in Flies, Fish, and Mice. *Cell* **174**, 481-496 e419 (2018).

- 480 11. Feng, J., *et al.* A Genetically Encoded Fluorescent Sensor for Rapid and Specific In Vivo
481 Detection of Norepinephrine. *Neuron* **102**, 745-761 e748 (2019).
- 482 12. Peng, Y., *et al.* 5-HT_{2C} Receptor Structures Reveal the Structural Basis of GPCR
483 Polypharmacology. *Cell* **172**, 719-730 e714 (2018).
- 484 13. Wan, Q., *et al.* Mini G protein probes for active G protein-coupled receptors (GPCRs) in
485 live cells. *J Biol Chem* **293**, 7466-7473 (2018).
- 486 14. Barnea, G., *et al.* The genetic design of signaling cascades to record receptor activation.
487 *Proc Natl Acad Sci U S A* **105**, 64-69 (2008).
- 488 15. Keene, A.C., *et al.* Diverse odor-conditioned memories require uniquely timed dorsal
489 paired medial neuron output. *Neuron* **44**, 521-533 (2004).
- 490 16. Waddell, S., Armstrong, J.D., Kitamoto, T., Kaiser, K. & Quinn, W.G. The amnesiac gene
491 product is expressed in two neurons in the Drosophila brain that are critical for memory. *Cell*
492 **103**, 805-813 (2000).
- 493 17. Lee, P.T., *et al.* Serotonin-mushroom body circuit modulating the formation of anesthesia-
494 resistant memory in Drosophila. *Proc Natl Acad Sci U S A* **108**, 13794-13799 (2011).
- 495 18. Yu, D., Keene, A.C., Srivatsan, A., Waddell, S. & Davis, R.L. Drosophila DPM neurons form
496 a delayed and branch-specific memory trace after olfactory classical conditioning. *Cell* **123**,
497 945-957 (2005).
- 498 19. Rudnick, G. & Wall, S.C. The molecular mechanism of "ecstasy" [3,4-methylenedioxy-
499 methamphetamine (MDMA)]: serotonin transporters are targets for MDMA-induced serotonin
500 release. *Proc Natl Acad Sci U S A* **89**, 1817-1821 (1992).
- 501 20. Liechti, M.E., Saur, M.R., Gamma, A., Hell, D. & Vollenweider, F.X. Psychological and
502 Physiological Effects of MDMA ("Ecstasy") after Pretreatment with the 5-HT₂ Antagonist
503 Ketanserin in Healthy Humans. *Neuropsychopharmacology* **23**, 396-404 (2000).
- 504 21. Hagino, Y., *et al.* Effects of MDMA on Extracellular Dopamine and Serotonin Levels in Mice
505 Lacking Dopamine and/or Serotonin Transporters. *Curr. Neuropharmacol.* **9**, 91-95 (2011).
- 506 22. Oikonomou, G., *et al.* The Serotonergic Raphe Promote Sleep in Zebrafish and Mice.
507 *Neuron* **103**, 686-701 e688 (2019).
- 508 23. Ren, J., *et al.* Anatomically Defined and Functionally Distinct Dorsal Raphe Serotonin Sub-
509 systems. *Cell* **175**, 472-487 e420 (2018).
- 510 24. Ren, J., *et al.* Single-cell transcriptomes and whole-brain projections of serotonin neurons
511 in the mouse dorsal and median raphe nuclei. *Elife* **8** (2019).
- 512 25. Kroeze, W.K., *et al.* PRESTO-Tango as an open-source resource for interrogation of the
513 druggable human GPCRome. *Nat Struct Mol Biol* **22**, 362-369 (2015).
- 514 26. Pfeiffer, B.D., Truman, J.W. & Rubin, G.M. Using translational enhancers to increase
515 transgene expression in Drosophila. *Proc Natl Acad Sci U S A* **109**, 6626-6631 (2012).
- 516 27. Dana, H., *et al.* Sensitive red protein calcium indicators for imaging neural activity. *Elife* **5**
517 (2016).
- 518 28. Gibson, D.G., *et al.* Enzymatic assembly of DNA molecules up to several hundred
519 kilobases. *Nat Methods* **6**, 343-345 (2009).
- 520 29. Yusa, K., *et al.* Targeted gene correction of alpha1-antitrypsin deficiency in induced
521 pluripotent stem cells. *Nature* **478**, 391-394 (2011).
- 522 30. Shin, M. & Venton, B.J. Electrochemical Measurements of Acetylcholine-Stimulated
523 Dopamine Release in Adult Drosophila melanogaster Brains. *Anal Chem* **90**, 10318-10325

- 524 (2018).
525 31. Wang, Q., Shui, B., Kotlikoff, M.I. & Sondermann, H. Structural Basis for Calcium Sensing
526 by GCaMP2. *Structure* **16**, 1817-1827 (2008).
527 32. Chen, T.W., *et al.* Ultrasensitive fluorescent proteins for imaging neuronal activity. *Nature*
528 **499**, 295-300 (2013).
529
530

Fig. 1



528 **Fig1: Design, optimization, and characterization of a novel genetically encoded 5-HT**
529 **sensor.**

530 **(a)** Left: schematic representation illustrating the principle behind the GRAB_{5-HT} sensor.
531 The crystal structures are from Protein Data Bank (PDB) archive (PDB ID: 6BQH and
532 6BQG for the inactive and active states of the 5-HT_{2C} receptor, respectively¹², and PDB ID:
533 3EVP for cpGFP³¹). Middle: the 5-HT sensor was optimized over 3 main steps, including
534 the cpGFP insertion site, the linker between cpGFP and 5-HT_{2C}, and critical amino acids
535 in cpGFP. Right: optimization of cpGFP and the engineering of 5-HTmut. The fluorescence
536 change in each candidate sensor is plotted against the brightness, with both axes
537 normalized to 5-HT1.0.

538 **(b)** Representative images (left), fluorescence traces (middle), and group data (right) of the
539 fluorescence response in neurons expressing 5-HT1.0 (green) or 5-HTmut (gray); where
540 indicated, 10 μ M 5-HT was applied; n = 12/3 (12 cells from 3 cultures) for each group.
541 Scale bar, 20 μ m.

542 **(c)** Kinetic analysis of the 5-HT1.0 sensor. Left, a representative image showing the
543 experiment protocol, in which the line-scanning mode was used to record the fluorescence
544 change in cells expressing 5-HT1.0 in response to local application of 5-HT, followed by
545 metergoline (Met) in the continued presence of 5-HT. Middle, representative traces
546 showing the rise and decay of 5-HT1.0 fluorescence in response to 5-HT (top) followed by
547 Met (bottom). Right, a summary of on and off kinetics of 5-HT1.0; n = 8/5 for each group.
548 Scale bar, 10 μ m.

549 **(d)** Summary of the change in fluorescence of 5-HT1.0 in response to 5-HT alone, 5-HT
550 together with Met or SB 252084 (SB), and 8 additional neurotransmitters and
551 neuromodulators. GABA, gamma-aminobutyric acid; Glu, glutamate; DA, dopamine; NE,
552 norepinephrine; ACh, acetylcholine; His, histamine; Oct, octopamine; and Gly, glycine; n =
553 3 wells per group with 300–500 cells per well.

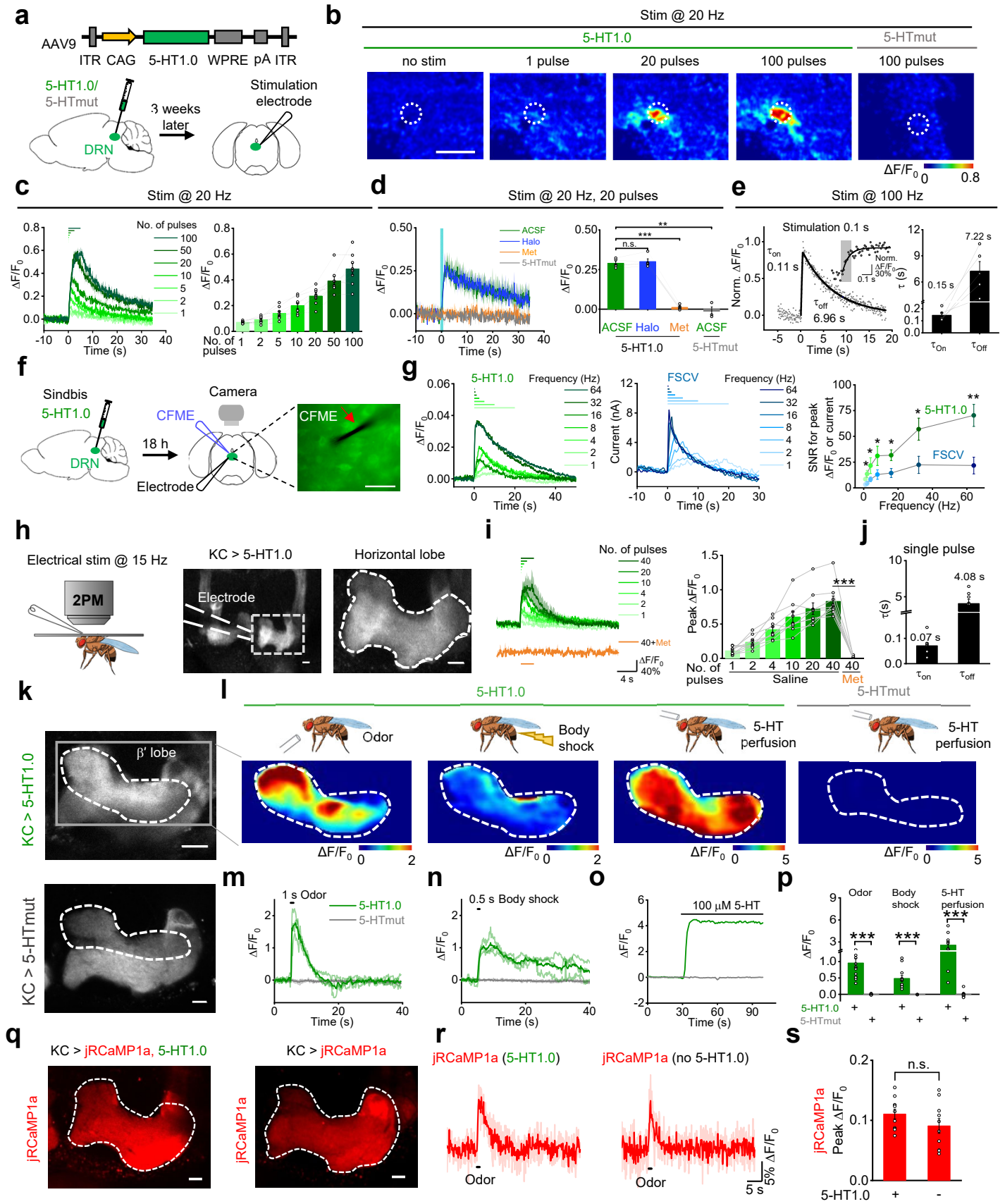
554 **(e)** Dose-response curve measured in neurons expressing 5-HT1.0 in response to
555 increasing concentrations of 5-HT, followed by Met; n = 18/4 for each group.

556 **(f, g)** G-protein coupling **(f)** and β -arrestin coupling **(g)** was measured for the 5-HT1.0
557 sensor and 5-HT_{2C} receptor using a luciferase complementation assay and TANGO assay,
558 respectively; n = 3 wells per group with 100-300 cells per well.

559 In this and subsequent figures, summary data are shown as the mean \pm SEM. *, $p < 0.05$,
560 **, $p < 0.01$, ***, $p < 0.001$, and n.s., not significant (Student's *t*-test).

561

Fig. 2



562 **Fig2: GRAB_{5-HT} can report the release of endogenous 5-HT in acute mouse brain**
563 **slices and *Drosophila*.**

564 **(a)** Schematic illustration depicting the mouse brain slice experiments. Top: The AAV vector
565 used to express the 5-HT1.0 sensor. Bottom: AAV expressing either 5-HT1.0 or 5-HTmut
566 was injected in the mouse DRN, after which acute brain slices were prepared and recorded.

567 **(b)** Representative pseudocolor images of the change in 5-HT1.0 and 5-HTmut
568 fluorescence in response to the indicated electrical stimuli delivered at 20 Hz. The duration
569 of one pulse is 1 ms. The white dotted circle (50 μm diameter) indicates the ROI used for
570 further analysis. Scale bar, 100 μm .

571 **(c)** Individual traces (left) and quantification (right) of 5-HT1.0 fluorescence change in
572 response to the indicated electrical stimuli delivered at 20 Hz; $n = 8$ slices from 5 mice.

573 **(d)** Representative traces (left) and group data of 5-HT1.0 and 5-HTmut fluorescence
574 change in response to electrical stimuli in slices treated with the dopamine receptor
575 antagonist haloperidol (Halo) or the 5-HT receptor antagonist Met; $n = 3-5$ slices from 2-4
576 mice.

577 **(e)** Left: normalized change in 5-HT1.0 fluorescence in response to 10 electrical stimuli
578 delivered at 100 Hz. The rise and decay phases are fitted with single-exponential functions
579 (black traces). A magnified view of the on kinetics in inset. Right: summary of τ_{on} and τ_{off} ; n
580 = 5 slices from 4 mice.

581 **(f)** Schematic drawing outlines the design of simultaneous imaging and fast-scan cyclic
582 voltammetry (FSCV) experiments in mouse DRN slice preparation. The red arrow indicates
583 that the carbon-fiber microelectrode (CFME) is placed near the neuron expressing 5-HT1.0.
584 Scale bar, 20 μm .

585 **(g)** Left: representative fluorescence traces of a DRN neuron expressing 5-HT1.0 to
586 electrical stimuli consisting of a train of 20 pulses at varied frequency. Middle: current vs
587 time traces of evoked 5-HT release at varied stimulating frequencies. Right: group
588 summary of the signal to noise ratio (SNR) of 5-HT1.0 and FSCV; $n = 11$ neurons from 9
589 mice.

590 **(h)** Left: schematic drawing showing *in vivo* two-photon imaging of a *Drosophila*, with the
591 stimulating electrode positioned near the mushroom body (MB). Middle and right:
592 representative images of a fly expressing 5-HT1.0 in the Kenyon cells (KCs) of the MB; the
593 image at the right is a magnified view of the dashed rectangle. The duration of one pulse
594 is 1 ms. Scale bar, 10 μm .

595 **(i)** Representative traces (left) and group analysis (right) of 5-HT1.0 fluorescence in
596 response to the indicated electrical stimuli in either saline (control) or 10 μM Met; $n = 9$ flies
597 for each group.

598 **(j)** Summary of 5-HT1.0 τ_{on} and τ_{off} in response to a single electrical stimulation; $n = 8$ flies
599 for each group.

600 **(k)** Fluorescence images measured in the MB of flies expressing 5-HT1.0 or 5-HTmut; the

601 β' lobe is indicated. Scale bar, 10 μm .

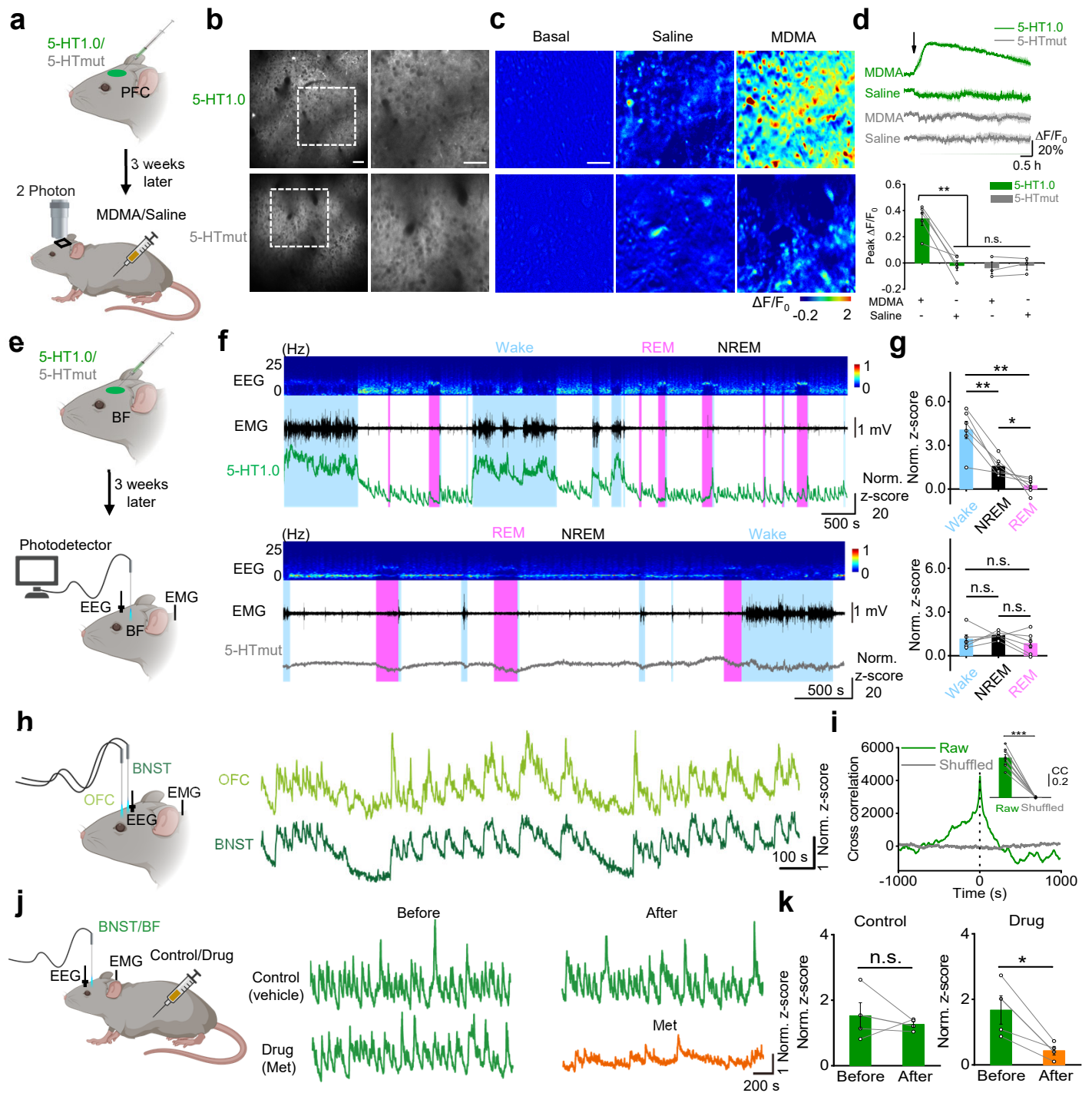
602 **(l-p)** Representative pseudocolor images **(l)**, fluorescence traces **(m-o)**, and group
603 summary **(p)** of 5-HT1.0 and 5-HTmut in the MB β' lobe measured in response to a 1-s
604 odor application, a 0.5-s body shock, and application of 100 μM 5-HT; n = 5-14 flies for
605 each group.

606 **(q)** Fluorescence images of jRCaMP1a in fly MB with co-expression of 5-HT1.0 (left) or
607 expressing jRCaMP1a alone (right) in the KCs. Scale bar, 10 μm .

608 **(r, s)** Representative traces **(r)** and group summary **(s)** of Ca^{2+} signal in the MB of flies co-
609 expressing jRCaMP1a and 5-HT1.0 or jRCaMP1a alone; where indicated, a 1-s odorant
610 stimulation was applied; n = 10-11 flies for each group.

611

Fig. 3



612 **Fig 3: GRAB_{5-HT} can report endogenous serotonergic activity in freely behaving mice.**

613 **(a)** Schematic diagram illustrating the use of two-photon imaging to measure 5-HT1.0 and
614 5-HTmut fluorescence in the prefrontal cortex (PFC) of head-fixed mice; MDMA or saline
615 was injected intraperitoneally.

616 **(b)** Representative images of 5-HT1.0 (top) and 5-HTmut (bottom) fluorescence measured
617 in the mouse PFC. Scale bar, 50 μ m.

618 **(c, d)** Representative pseudocolor images **(c)**, averaged fluorescence traces **(d, top)**, and
619 group summary **(d, bottom)** showing 5-HT1.0 (top, green) and 5-HTmut (bottom, gray)
620 fluorescence measured after an i.p. injection of saline (middle) or 10 mg/kg MDMA (right);
621 n = 3-5 mice for each group. Scale bar, 50 μ m.

622 **(e)** Schematic diagram illustrating the use of fiber-photometry for measuring 5-HT1.0 and
623 5-HTmut fluorescence in the basal forebrain (BF) of freely behaving mice during the sleep-
624 wake cycle. EEG and EMG were also measured.

625 **(f)** Representative EEG, EMG, and 5-HT1.0 (top panel) and 5-HTmut (bottom panel)
626 fluorescence measured during the sleep-wake cycle.

627 **(g)** Summary of 5-HT1.0 (top) and 5-HTmut (bottom) fluorescence measured in awake
628 mice and during NREM and REM sleep; n = 3 mice in two sessions for each group.

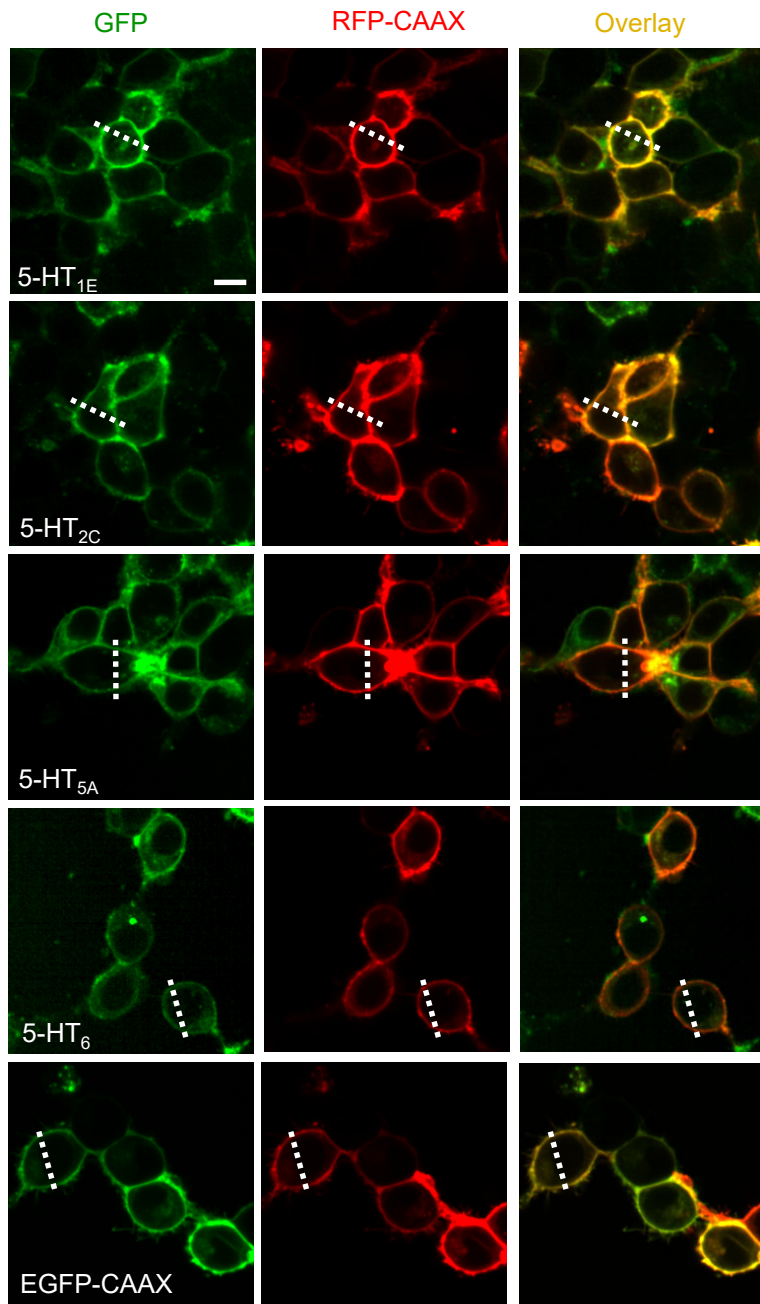
629 **(h, i)** Same as in **(e)**, except the 5-HT1.0 sensor was expressed in both the orbital frontal
630 cortex (OFC; light green) and the bed nucleus of the stria terminalis (BNST; dark green),
631 and the fluorescence response in each nucleus was recorded and analyzed. The cross-
632 correlation between the signals in the OFC and BNST is shown in **(i)**; n = 4 mice in two
633 sessions for each group.

634 **(j, k)** 5-HT1.0 fluorescence was measured in the BNST and BF as in **(h)**; where indicated,
635 the mice received an injection of saline (control) or Met. The normalized responses in the
636 BNST (n = 3 mice) and BF (n = 1 mouse) were combined for the group summary.

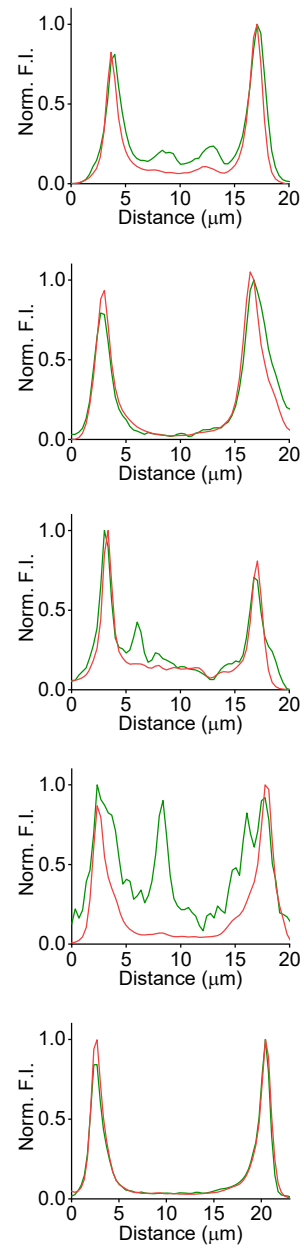
637

Extended Data Fig. 1

a



b



638 **Extended Data Fig. 1: Characterization of the membrane trafficking for 5-HT**
639 **receptor- based chimeras (related to Fig. 1).**

640 **(a)** Representative fluorescence images of HEK293T cells co-expressing the indicated 5-
641 HT receptors fused with cpGFP (green) and RFP-CAAX (red); EGFP-CAAX was used as
642 a positive control. Scale bar, 10 μm .

643 **(b)** Normalized fluorescence intensity measured at the white dashed lines shown in **(a)**
644 for each candidate sensor.

645

Extended Data Fig. 2

a



b

1 METDTLLLVVLLLVVPGSTGDTSLYKKVGTGTVNLRNAVHSFLVHLIGLL 50
51 VWQCDISVSPVAAIVTDIFNTSDGGRFKFPDGVQNWPAISIVIIIMTIG 100
101 GNILVIMAVSMEKKLHNATNYFLMSLAADMLVGLLVMPLSLLAILYDYV 150
151 WPLPRYLCPVWISLDVLFSTASIMHLCAISLDRYVAIRNPIEHSRFNSRT 200
201 KAIMKIAIVWAISIGVSVPIPVIGLRDEEKVFNNTTCVLN DPNFVLI GS 250
251 FVAFFIPLTIMVITYCLTIYVLRQALMFLNG NVYIKADKQKNGIKANFH 300
301 IRHNIEDGGVQLAYHYQQNTPIGDGPVLLPDNHVLSVQSKLSKDPNEKRD 350
351 HMLLEFVTAAGITLGMDELYKGGTGG QESMS SKGEELFTGVVPILEVELD 400
401 GDVNGHKFSVSGEGEGDAT T GKLT LKFICTTGKLPVPWPPTLVTTLT YGVQ 450
451 CFSRYPDHMKQHDFFKSAMPEGYIQERTIFFKDDGNYKTRAEVKFEGDTL 500
501 VNRIELKGI DFKEDGNILGHKLEYN GFATA NNERKASKVLGIVFFVFLIM 550
551 WCPFFITNILSVLC EKSCNQKLMEKLLNVFVWIGYVCSGINPLVYTLFNK 600
601 IYRRAFS NYLRCNYKVEKKPPVRQIPRVAATALS GRELVNIYRHTNEPV 650
651 IEKASDNEPGIEMQVENLEL P VNPSSVVSERISSV * 700

646 **Extended Data Fig. 2: The amino acids sequence of 5-HT1.0 (related to Fig. 1).**

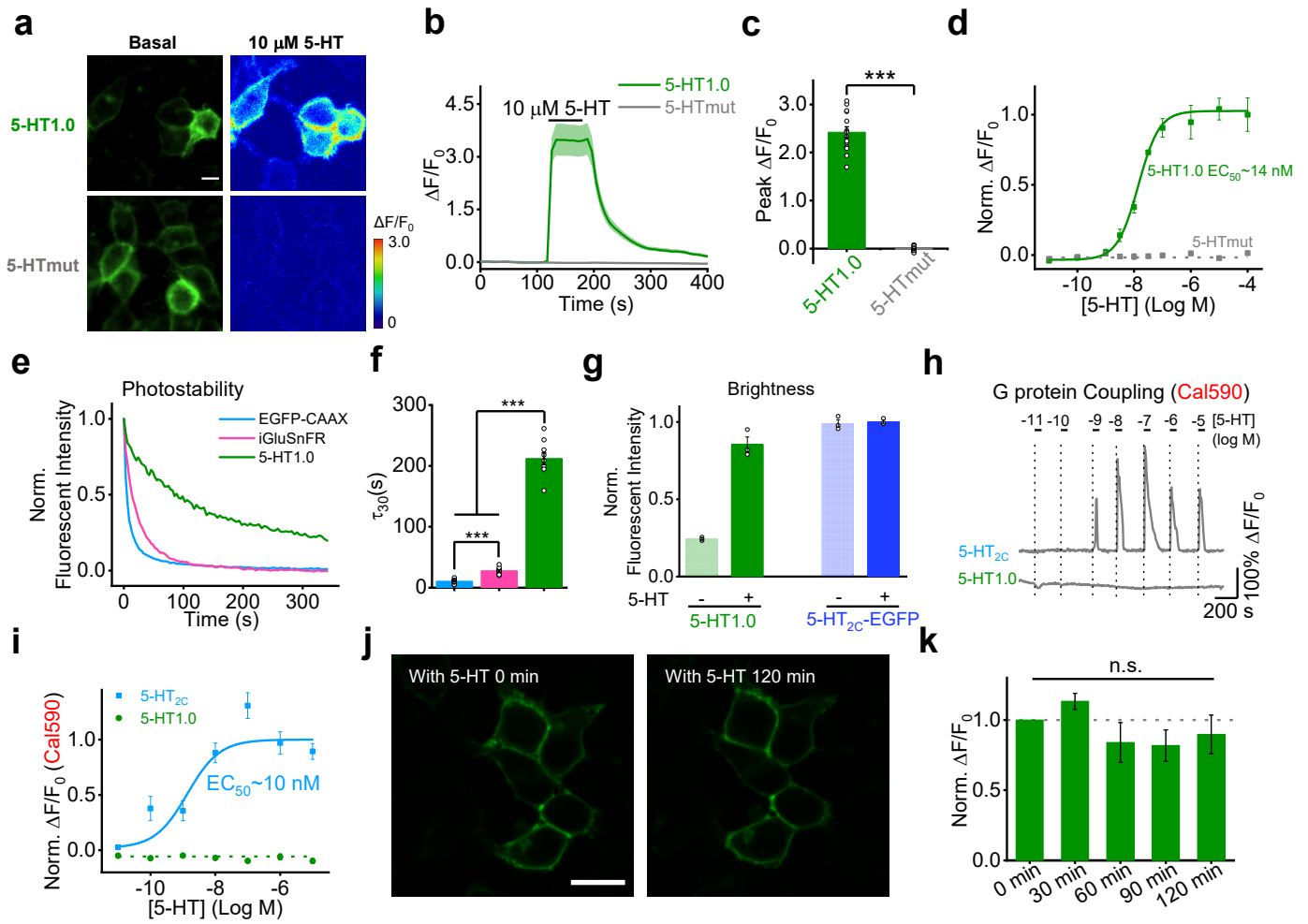
647 **(a)** Schematic representation of the 5-HT1.0 structure. For simplicity TM1-4, TM7 and H8
648 are not shown.

649 **(b)** Amino acids sequence of the 5-HT1.0 after three steps evolution. The mutated amino
650 acids in cpGFP (cpGFP from GCaMP6s³²) are indicated in red box.

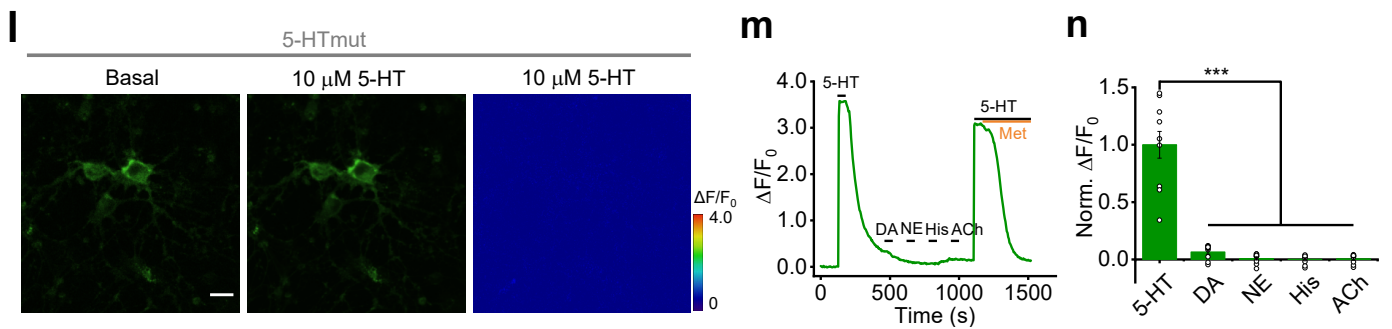
651

Extended Data Fig. 3

Characterization in cultured HEK293T cells



Characterization in cultured neurons



652 **Extended Data Fig. 3: Further characterization of GRAB_{5-HT} in cultured HEK293T**
653 **cells and neurons (related to Fig. 1).**

654 **(a)** Representative fluorescence and pseudocolor images of HEK293T cells expressing 5-
655 HT1.0 or 5-HTmut before (left) and after (right) application of 10 μ M 5-HT. Scale bar, 20
656 μ m.

657 **(b, c)** Representative fluorescence traces and group summary of the peak response in
658 HEK293T cells expressing 5-HT1.0 or 5-HTmut; n = 14-15 cells from 3 cultures for each
659 group.

660 **(d)** 5-HT dose-response curves measured in cells expressing 5-HT1.0 or 5-HTmut, the
661 EC₅₀ for 5-HT1.0 is shown.

662 **(e)** Representative normalized fluorescence measured in cells expressing 5-HT1.0, EGFP-
663 CAAX, or iGluSnFR during continuous exposure to 488-nm laser (power: 350 μ W).

664 **(f)** Summary of the decay time constant calculated from the photobleaching curves shown
665 in **(e)**. n = 10/3, 14/3, and 12/3 for 5-HT1.0, EGFP-CAAX, and iGluSnFR, respectively.

666 **(g)** Summary of the brightness measured in cells expressing 5-HT1.0 or 5-HT_{2C}-EGFP in
667 the absence or presence of 10 μ M 5-HT, normalized to the 5-HT_{2C}-EGFP + 5-HT group; n
668 = 3 wells per group with 300–500 cells per well.

669 **(h, i)** Intracellular Ca²⁺ measured in cells expressing 5-HT1.0 or the 5-HT_{2C} receptor and
670 loaded with the red fluorescent calcium dye Cal590. Representative traces are shown in
671 **(h)**, and the peak responses are plotted against 5-HT concentration in **(i)**; n = 15/3 for each
672 group.

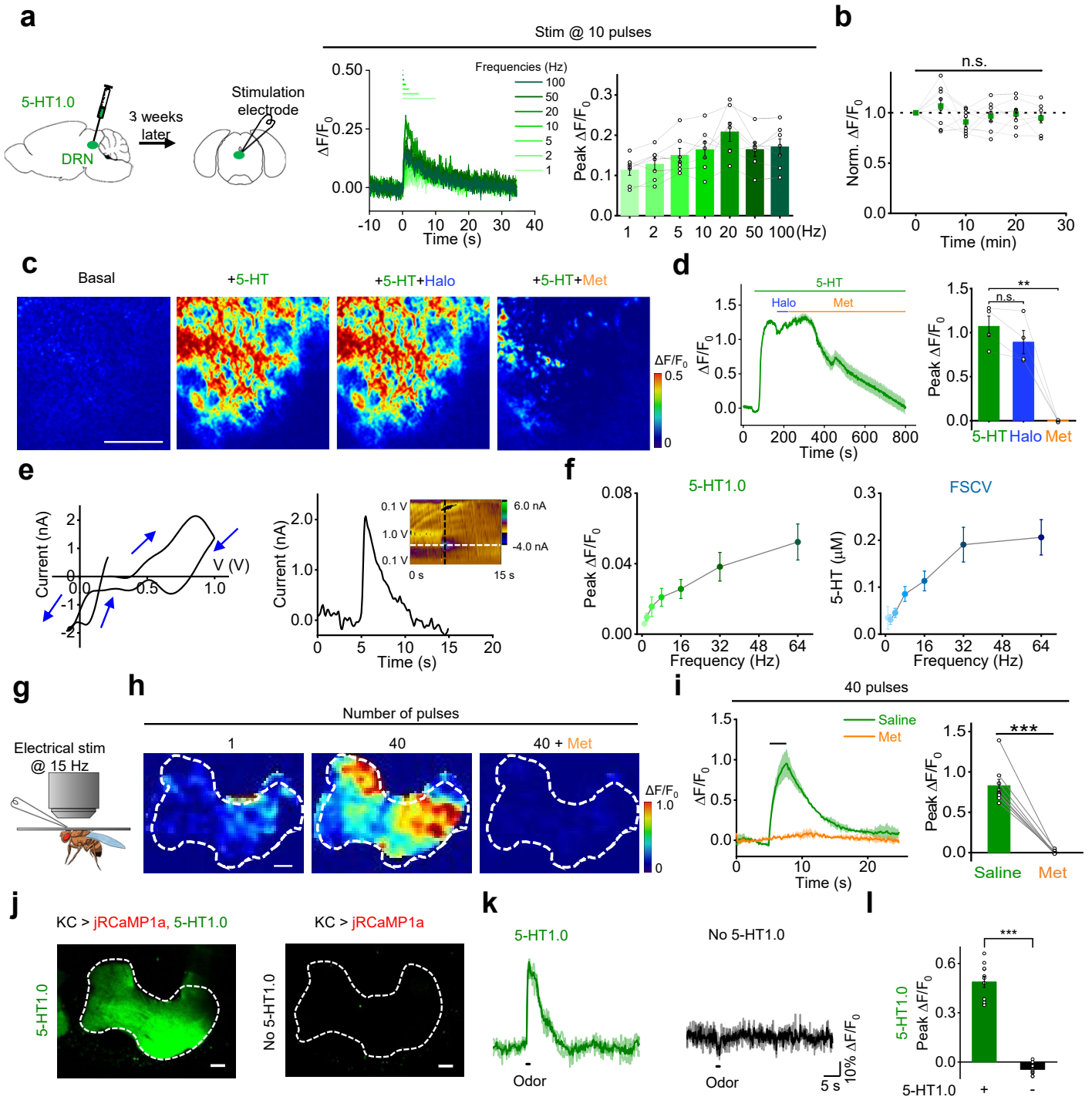
673 **(j, k)** Fluorescence response of 5-HT1.0 expressing cells to 5-HT perfusion for two hours.
674 Representative fluorescence images **(j)** and the summary data **(k)** showing the response
675 to 10 μ M 5-HT applied at 30 min intervals to cells expressing 5-HT1.0; n = 3 wells per group
676 with 100-300 cells per well. Scale bar, 20 μ m.

677 **(l)** Cultured cortical neurons expressing the 5-HTmut sensor were imaged before (left) and
678 after (middle) 5-HT application. The pseudocolor image at the right shows the change in
679 fluorescence. Scale bar, 20 μ m.

680 **(m, n)** Representative trace **(m)** and group summary **(n)** of cultured neurons expressing 5-
681 HT1.0 in response to indicated compounds at 10 μ M each; in **(m)**, Met was applied where
682 indicated; n = 9/3.

683

Extended Data Fig. 4



684 **Extended Data Fig. 4: Probing endogenous 5-HT release in mouse brain slices and**
685 ***Drosophila in vivo* (related to Fig. 2).**

686 **(a)** Left: schematic diagram depicting the acute mouse brain slice preparation, with AAV-
687 mediated expression of 5-HT1.0 in the DRN. Middle and right: fluorescence traces (middle)
688 and group data (right) of the change in 5-HT1.0 fluorescence in response to 10 electrical
689 stimuli applied at the indicated frequencies; n = 7 slices from 5 mice.

690 **(b)** Summary of the change in 5-HT1.0 fluorescence in response to 6 trains of electrical
691 stimuli (20 pulses at 20 Hz) delivered at 5-min intervals. The responses are normalized to
692 the first train; n = 8 slices from 5 mice.

693 **(c, d)** Representative pseudocolor images **(c)**, fluorescence traces **(d, left)**, and group data
694 **(d, right)** of 5-HT1.0 fluorescence in response to perfusion of 5-HT, 5-HT+Halo, and 5-
695 HT+Met; n = 4 slices from 3 mice for each group.

696 **(e)** Left: representative FSCV data of 5-HT release in DRN. A specific 5-HT waveform (0.2
697 V to 1.0 V and ramped down to -0.1 V, and back to 0.2 V at a scan rate of 1000 V/s) was
698 applied to the CFME at a frequency of 10 Hz. Right: current vs time traces is extracted at
699 horizontal white dashed line shows immediate increase in 5-HT response after electrical
700 stimulation (20 pulses, 2 ms pulse width, 64 Hz). A cyclic voltammogram (inset) is extracted
701 at the vertical black dashed line shows oxidation and reduction peaks at 0.8 V and 0 V,
702 respectively.

703 **(f)** Left: group data of fluorescence response in 5-HT1.0-expressing DRN neurons to
704 electrical stimuli with varied frequency delivered at 20 pulses. Right: average data of peak
705 5-HT concentration measured by FSCV at varied stimulating frequencies; n = 11 neurons
706 from 9 mice.

707 **(g)** Schematic drawing showing *in vivo* two-photon imaging of a *Drosophila*, with the
708 stimulating electrode positioned near the mushroom body (MB).

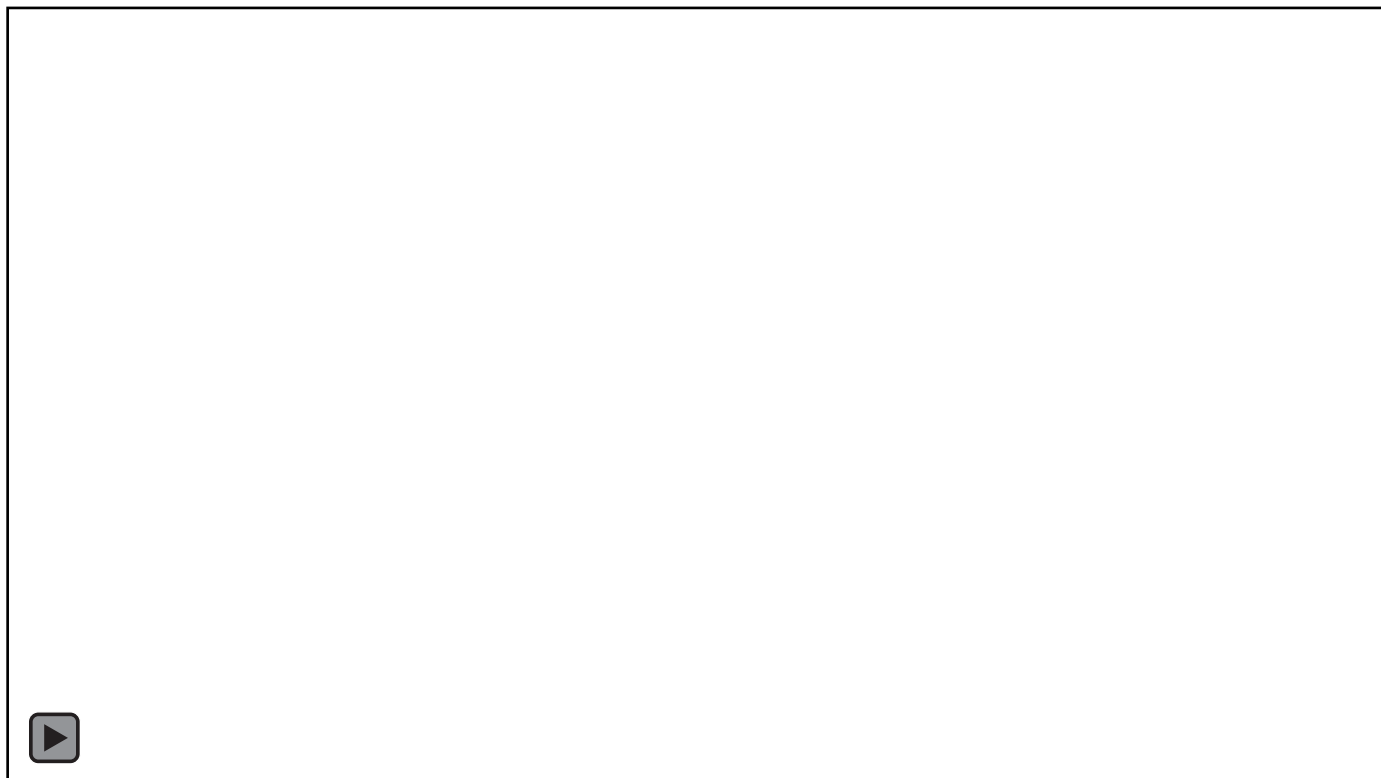
709 **(h, i)** Representative pseudocolor images **(h)**, fluorescence traces and group summary **(i)**
710 of the change in 5-HT1.0 fluorescence in the MB horizontal lobe in response to 40 electrical
711 stimuli at 15 Hz in control (saline) or 10 μ M Met; n = 9 flies for each group. Scale bar, 10
712 μ m.

713 **(j)** Fluorescence images of green channel of MB in flies with co-expression of jRCaMP1a
714 and 5-HT1.0 (left) or expressing jRCaMP1a alone (right) in the KCs. Scale bar, 10 μ m.

715 **(k, l)** Representative traces **(k)** and group summary **(l)** of 5-HT signal in the MB of flies co-
716 expressing jRCaMP1a and 5-HT1.0 or jRCaMP1a alone; where indicated, a 1-s odorant
717 stimulation was applied; n = 10-11 flies for each group.

718

Extended Data video 1



719 **Extended Data video 1 GRAB_{5-HT} reports the sensory-relevant 5-HT release in**
720 ***Drosophila* (Related to Fig. 3k-p).**

721 Fluorescence responses of 5-HT1.0 and 5-HTmut in the MB β' lobe measured in response
722 to a 1-s odor application, a 0.5-s body shock, and application of 100 μ M 5-HT.